A PERSISTENT HIGH-ENERGY FLUX FROM THE HEART OF THE MILKY WAY: INTEGRAL'S VIEW OF THE GALACTIC CENTER[*]

G. B´   [1,2], A. G   [1,2], M. R   [1,2], R. T   [1,2], F. M   [3], N. L   [4], J. P   [1,2], G. S   [5], F. Y   -Z   [6]

ABSTRACT

Highly sensitive imaging observations of the Galactic center (   ) at high energies with an angular resolution of order 10 arcminutes, is a very recent development in the field of high-energy astrophysics. The Ibis/Isgri imager on the *Integral* observatory detected for the first time a hard X-ray source, IGR J17456–2901, located within 1 arcminute of Sagittarius A* (Sgr A*) over the energy range 20–100 keV. Here we present the results of a detailed analysis of approximately 7×10^6 s of observations of the   obtained since the launch of *Integral* in October 2002. Two years and an effective exposure of 4.7×10^6 s have allowed us to obtain more stringent positional constraints on this high-energy source and to construct its spectrum in the range 20–400 keV. Furthermore, by combining the Isgri spectrum together with the total X-ray spectrum corresponding to the same physical region around Sgr A* from *XMM-Newton* data, and collected during part of the gamma-ray observations, we constructed and present the first accurate wide band high-energy spectrum for the central arcminutes of the Galaxy. Our complete and updated analysis of the emission properties of the *Integral* source shows that it is faint but persistent with no variability above 3σ, contrary to what was alluded to in our first paper. This result, together with the spectral characteristics of the soft and hard X-ray emission from this region, suggests that the source is most likely not point-like but, rather, that it is a compact, yet diffuse, non-thermal emission region. The centroid of IGR J17456–2901 is estimated to be R.A. = $17^h45^m42^s.5$, decl. = $-28°59'28''$ (J2000), offset by 1′ from the radio position of Sgr A* and with a positional uncertainty of 1′. Its 20–400 keV luminosity at 8 kpc is $L = (5.37 \pm 0.21) \times 10^{35}$ erg s^{-1}. A 3σ upper limit on the flux at the electron-positron annihilation energy of 511 keV from the direction of Sgr A* is set at 1.9×10^{-4} ph cm^{-2} s^{-1}. Very recently, the *Hess* collaboration presented the detection of a source of $\sim$ TeV γ-rays also located within an arcminute of Sgr A*. We present arguments in favor of an interpretation according to which the photons detected by *Integral* and *Hess* arise from the same compact region of diffuse emission near the central black hole and that the supernova remnant Sgr A East could play an important role as a contributor of very high-energy γ-rays to the overall spectrum from this region. There is also evidence for hard emission from a region located between the central black hole and the radio Arc near l $\sim 0.1°$ along the Galactic plane and known to contain giant molecular clouds.

Subject headings: black hole physics — Galaxy: center — Galaxy: nucleus — X-rays: observations — stars: neutron — X-rays: binaries

1. INTRODUCTION

The year 2004 marked the 30th anniversary of the discovery of the compact radio source Sgr A* (Balick & Brown 1974), which is now firmly believed by many to be the manifestation of a supermassive black hole that sits at the very heart of the Milky Way and around which everything in the Galaxy turns. That year also marked the first detection of γ-rays from a compact region of size $\sim$ 10 arcminutes around Sgr A* with the *Integral* observatory in the energy range from 20 to 100 keV (Bélanger et al. 2004) and with the *Hess* Cerenkov telescope array between 165 GeV and 10 TeV (Aharonian et al. 2004). After three decades of observations, we finally detected a source of very high-energy radiation that appears to be point-like and coincident with the Galactic nucleus (   ). However, the exact nature of the highly energetic emission from this com-

pact region is unknown. Our aim here is to present observational evidence that will lead to a deeper understanding of the emission process, and help to unfold the mystery of the γ-rays arriving from the heart of the Milky Way.

The Galactic nuclear region is very dense and complex — so dense that certainly more than one source could contribute to the high-energy flux detected by present-day γ-ray instruments with typical angular resolutions of 10–15 arcminutes. Located at 8 kpc from the Sun, the Galactic center (   ) harbours a supermassive black hole whose presence and mass of about 3.6×10^6 M$_\odot$ were deduced primarily from near-infrared (   ) observations and measurements of the velocity and proper motion of the stars contained in the central cluster (Schödel et al. 2003; Ghez et al. 2005; Eisenhauer et al. 2005). A black hole (   ) of this mass has a Schwarzschild radius (R_S) of about 1.2×10^{12} cm and is expected to accrete the matter from its nearby environment producing a detectable emission in a broad range of frequencies (Melia & Falcke 2001). The bright, compact, non-thermal radio source Sgr A*, located at less than $0''.01$ from the dynamical center of the central star cluster, is most likely the manifestation of such accretion processes. Undetectable in the visible and   bands due to the large Galactic absorption, and only recently detected in   both in quiescent, and flaring states (Genzel et al. 2003; Ghez et al. 2004), this source is surprisingly weak in X-rays, where it appears slightly extended with a luminosity of only $L_X[2\text{–}10\,\text{keV}] \approx 2 \times 10^{33}$ erg s^{-1} (Baganoff et al. 2003).

The dense central region of the Milky Way where the 2–10 keV flux is heavily dominated by diffuse radiation, includes the emission from a hot ($kT \sim 6$–8 keV) probably unbound thermal plasma component, the supernova remnant ( ) Sgr A East, several knots and filaments, and thousands of point sources (Maeda et al. 2002; Park et al. 2004; Muno et al. 2004a; Muno et al. 2004b). The faint X-ray counterpart of Sgr A* would likely have gone unnoticed were it not positioned almost exactly at the centre of the Galaxy.

Following a monitoring of this faint X-ray source by the *Chandra* observatory, it was discovered that Sgr A* is the site of sometimes powerful X-ray flares (Baganoff et al. 2001). This flaring activity was also detected and studied with *XMM-Newton* (Goldwurm et al. 2003a; Porquet et al. 2003a; Bélanger et al. 2005) and the peak luminosity during these flares was seen to rise above quiescence by factors up to 180 and then decay in a few hours or less. The majority of flares have spectra that are significantly harder (power law photon index $\Gamma \sim 1.5$) than the quiescent spectrum ($\Gamma \sim 2.7$), but the most powerful of them was quite soft ($\Gamma \sim 2.5$). Note that dust scattering can have some effect on the observed fluxes and spectral indeces of both the quiescent and flaring states of Sgr A* (Tan & Draine 2004). Variations on time scales as short as 200 s have been detected during flares indicating an emitting region with a size of the order of $10 R_S$. Recent *Chandra* and *XMM-Newton* campaigns have allowed us to estimate the average X-ray flare rate to about 1 per day bearing in mind that the flaring events appear to be clustered (Bélanger et al. 2005). At slightly longer wavelengths, observations with the *VLT* Naco imager (Genzel et al. 2003) and *Keck* telescope (Ghez et al. 2004) have shown that Sgr A* is also the source of frequent flares with durations comensurable with those seen in X-rays. Some flares even appear to be simultaneous with X-ray flares (Eckart et al. 2004). Both the and X-ray flaring events strongly suggest the presence of an important population of non-thermal relativistic electrons in the vicinity of the horizon (Markoff et al. 2001; Liu & Melia 2002; Yuan et al. 2002; Yuan et al. 2003; Liu et al. 2004) and therefore their detection has raised great interest in the possibility of observing hard X-rays from the Galactic nucleus.

Sgr A*'s bolometric luminosity from radio to X-rays (including the flares) barely amounts to a few 10^{36} erg s^{-1}, while the Eddington luminosity for a of its mass reaches $L_E \approx 4 \times 10^{44}$ erg s^{-1}. Even the expected accretion luminosity, based on an estimated stellar wind mass rate at the accretion radius, is of the order of 10^{42-43} erg s^{-1}, i.e. about 6 to 7 orders of magnitude higher than Sgr A*'s total observed emitted power (see Cuadra et al. 2005 for a recent update on the issue).

In the 1990's it was thought that the bulk of the power could be found at higher energies; in hard X-rays as is the case for binaries in the hard state, or even at the electron-positron annihilation energy of 511 keV (see e.g. Genzel & Townes 1987). Other than the detections in the 10–20 keV range from the direction of the based on /*Spacelab 2* (Skinner et al. 1987) and Art-P/*Granat* (Pavlinsky et al. 1994) data, no detection at energies above 20 keV emanating from Sgr A complex was reported. A long monitoring of the region by the Sigma telescope on the *Granat* satellite yielded upper limits of the order of several 10^{35} erg s^{-1} to the 35–150 keV emission from Sgr A* (Goldwurm et al. 1994; Goldoni et al. 1999), and 2.3×10^{-4} ph cm^{-2} s^{-1} to the flux at 511 keV from a point source at the (Malet et al. 1995).

In the 100 MeV to 10 GeV energy range, an unidentified γ-ray source of the *Egret*/ catalog 3EG J1746–2851, was found to be somewhat compatible with the

(Mayer-Hasselwander et al. 1998). In the third *Egret* catalog (Hartman et al. 1999), this source is located 0.17° from Sgr A* and the reported error radius is 0.13° at 90% confidence level. Taking this at face value would marginally exclude Sgr A*. However, given the 1° angular resolution of the instrument and hence its inability to exclude the contribution from other sources contained in a region of this size, 3EG J1746–2851 is still considered as possibly coincident with the .

Finally, *Integral* observations performed during the first half of 2003 with the Ibis telescope revealed for the first time the presence of a significant excess in the energy range 20–100 keV coming from the inner region of the Galaxy (Bélanger et al. 2004). The position of this excess was found to lie 1′ from Sgr A* with a 4′ error radius, and its luminosity was estimated to be $L_X[20\text{–}100 \text{ keV}] \approx 3 \times 10^{35}$ erg s^{-1}. An indication of variability on timescales comparable to those of flares in Sgr A* was reported but a subsequent analysis that included data collected over the second half of 2003 with improved analysis procedures found the source to be stable (Goldwurm et al. 2004). In 2003 June, *Chandra* detected two new transient sources in the close vicinity of Sgr A*. Given the 12′ resolution of the Ibis/*Integral* telescope, the possibility that the 20–100 keV excess was linked to the emission from these objects, was considered and discussed in Bélanger et al. (2004).

Meanwhile the *Hess* collaboration (Aharonian et al. 2004) announced the detection of a bright source of TeV photons coincident with Sgr A* to within 1′. The source appears to be point-like, stable, with a power-law spectrum of index of 2.2 and a luminosity of $L_\gamma[1\text{–}10 \text{ TeV}] \approx 10^{35}$ erg s^{-1}.

This wealth of high-energy data all point to the presence of one, or several, high energy non-thermal emission components likely produced by accelerated particles in the environment of the . Both leptonic and hadronic origins for the accelerated particles giving rise to the γ-rays have been considered either in the inner (Markoff et al. 1997; Aharonian & Neronov 2005) or outer (Atoyan & Dermer 2004) region of Sgr A*, while Melia et al. (1998), Fatuzzo & Melia (2003) and recently Crocker et al. (2005), discussed the possibility that the site of particle acceleration could be the unusual supernova remnant Sgr A East.

Sgr A East is a mixed morphology whose center is at less than 1′ from Sgr A* and whose radio shell spans a few arcminutes. Given its position and dimensions it would appear like a stable point-like source for γ-ray observatories. This remnant is characterised by a non-thermal radio shell at the center of which lies an apparently ejecta-dominated X-ray emiting region whose spectrum indicates that the plasma is rich in heavy elements especially towards the core where Fe abundances reach 4–5 times solar (Maeda et al. 2002; Sakano et al. 2004). For this reason, it has been classified as a metal-rich mixed morphology . The fact that Sgr A East is the smallest of the known s of this type and that its radio shell appears to be quite symmetrical, although slightly elongated along the Galactic plane, suggests that the ejecta from the explosion have expanded in a very dense but more or less homogenous environment (Maeda et al. 2002). According to a more recent analysis of the X-ray features of Sgr A East by Sakano et al. (2004) based on *XMM-Newton* observations, the derived total energy, mass and abundance pattern are consistent with a single supernova event of Type Ia or Type II involving a relatively low-mass progenitor star. Furthermore, according to these authors the morphology and spectral characteristics do not show evidence of a clear connection between the and past activity in Sgr A*.

Sgr A East may very well have arisen from a single explosion akin to most other supernova events in terms of its energetics

as is suggested by Sakano et al. (2004). The most recent simulations for its genesis and evolution (Fryer et al. 2005) indicate that the progenitor was likely a star of mass $\sim 15\,M_\odot$ that exploded a mere ~ 1750 years ago. Reaching the M-0.02-0.07 cloud some 300–400 years ago, the expanding shock collided with the dense molecular gas, producing a bright flash of 2–200 keV emission lasting several hundred years, whose X-ray echo we may be viewing today in the form of Fe fluorescent emission from Sgr B2 (and other nearby clouds). However, Sgr A East does distinguish itself from other Galactic remnants in three important ways. First, it is located very near the , within 50″ of Sgr A*, and is therefore subject to interactions and forces uncommon in the rest of the Galaxy. Second, its non-thermal shell emission caused by synchrotron radiation from relativistic electrons has an unusually high surface brightness compared to other Galactic (Green 2004). Third, OH (1720 MHz) maser emission detected in several locations around the , and particularly at the boundary of Sgr A East and the M-0.02-0.07 molecular cloud, indicates the presence of strong shocks where rapid acceleration of electrons (and protons) is taking place, in a medium threaded by very strong magnetic fields of order 2–4 mG (Yusef-Zadeh et al. 1996). As pointed out by Yusef-Zadeh, Melia & Wardle (2000), the presence of relativistic electrons and strong magnetic fields within Sgr A East makes it a unique and potentially powerful Galactic accelerator.

Other possible sources of non-thermal γ-rays, some of which were initially proposed to explain certain features of the X-ray emission like the hot component and the bright 6.4 keV line of neutral Fe, or the non-thermal radio characteristics of the region, include the radio Arc, several non-thermal filaments and regions marked by cosmic ray electron interactions (Yusef-Zadeh et al. 2002), supernova ejecta (Bykov 2002), and scattering of highly energetic radiations from molecular clouds. In particular Revnivtsev et al. (2004) proposed a model in which the *Integral* source IGR J17475–2822, coincident with the dense molecur cloud Sgr B2, is due to Compton reflection (i.e. the scattering of high-energy photons by cold electrons in the outer layers of the cloud) of very energetic emission from a very powerful flare in the Sgr A* system about 300 years ago. In any case, none of the current models can integrate the three high-energy sources (IGR J17456–2901, 3EG J1746-2851, HESS J1745–290) detected near the in a comprehensive manner.

We report here a complete study of the 2003-2004 *Integral*/Ibis data of the aiming to clearly depict the morphology of this interesting region at energies 20 to 400 keV, and to present the properties of the central source IGR J17456–2901. The *Integral* observatory monitored the region for all of 2003 and 2004, including some dedicated programs specifically planned to study the properties of the . An important goal of this study was to search for correlated variability between the X-rays from Sgr A* and the higher energy emission from the central *Integral* source.

We describe the observations and data reduction methods in sections 2 and 3. Our results are presented in § 4 and include those of the multi-wavelength campaign on Sgr A* performed in 2004 pertaining to *Integral* (§ 4.4). Finally, we discuss some of their implications in § 5.

2. OBSERVATIONS

The *Integral* observatory carries two main γ-ray instruments; Ibis and Spi, working in the energy range 15 keV to 10 MeV (Winkler 2003). Since its launch, *Integral* has observed the central degrees of our Galaxy for a total of about 7 Ms. This

TABLE 1
O   L

	Obs Start time (UT)	Obs End time (UT)	Pointings	Exposure (Ms)
2003 Spring [a]	2003-02-28	2003-04-22	413	0.67
2003 Fall [b]	2003-08-18	2003-10-16	805	2.20
2004 Spring	2004-02-07	2004-04-21	550	1.01
2004 Fall	2004-08-28	2004-09-17	262	0.53

[a]Loosely used to designate the first part of the year
[b]Used to designate the second part of the year

time was divided between the Galactic Center Deep Exposure and Galactic Plane Scan core programs, and Guest Observer ( ) observations. In particular we include here analysis of programs performed in 2003 and in 2004 specifically dedicated to the . The 2004 program (~ 600 ks) was part of a broad multiwavelength campaign driven by a *XMM-Newton* large project aimed to study the flaring activity of Sgr A*.

The data that form the basis of this paper constitute a subset of all these observations selected such that the aim point is within $10°$ of the central . We have performed a detailed analysis of 2174 pointings carried out between the end of February 2003 and October 2004. Each pointing or science window (ScW) typically lasts between 1800–3600 s during which the telescopes are aimed at a fixed direction in the sky. Table 1 gives a summary of the overall periods spanned by the observations.

With a total effective exposure time of 4.7 Ms at the position of Sgr A*, we have constructed high signal-to-noise images of the central degrees and the spectrum of the central source IGR J17456–2901 first detected by *Integral* in 2003 (Bélanger et al. 2004). The results presented here are based on data collected with the Ibis/Isgri telescope (Ubertini et al. 2003; Lebrun et al. 2003) sensitive in the energy range between 15 and 1000 keV. The angular resolution of the high-energy (15 keV–10 MeV) Spi telescope ($\sim 3°$) is not sufficient to resolve the contribution of the high-energy sources known to be present in the central degrees of the Galaxy and we have therefore not used these data.

The X-ray monitor on-board *Integral*, Jem-X, has a smaller field of view than Ibis and Spi and therefore the effective exposure at the location of Sgr A* is substantially lower (~ 350 ks for the dataset considered in this paper). We analyzed the Jem-X data to produce mosaics for the and discuss the results below.

We have also made use of *XMM-Newton* data from the multi-wavelength campaign on Sgr A* carried out in 2004 to construct the broadband high-energy spectrum of IGR J17456–2901, and to identify the X-ray and soft γ-ray components. A detailed description of the *XMM-Newton* observations during this campaign, and of the characteristics of the two factor-40 flares detected from the direction of Sgr A* are presented in Bélanger et al. (2005).

3. DATA ANALYSIS METHODS

The basic Ibis/Isgri data reduction for individual pointings was performed using the *Integral* Off-line Scientific Analysis software ( ) version 4.2 delivered by the (Courvoisier et al. 2003) and whose algorithms are described in Goldwurm et al. (2003b) and Gros et al. (2003). Following the recommendations related to the use of the software, we restricted our analysis to events with energies greater than 20 keV. A number of additional procedures were implemented

in order to maximize the quality of our analysis given the large data set and the complexity of Galactic nuclear region. For instance, the analysis was consistently done twice: a first time to make a catalog of detected sources and perform a preliminary evaluation of the quality of each sky image, and a second time to ensure that all known sources in a given field of view were modeled correctly in the reconstruction of each sky image. The total number of sources detected by Isgri within $10°$ of the   , and therefore included in the analysis input catalog is 80. The background maps were constructed from empty field observations at high latitudes in 256 bands from 17 to 1000 keV and incorporated in the standard analysis where they were combined to match the chosen energy ranges. This procedure has allowed us to achieve the best possible quality for individual sky images and thus for the mosaic and spectrum. Other additional analysis procedures are detailed in the sections that follow.

3.1. *Sky maps, light curves and mosaics*

For a coded mask instrument like Ibis, a sky image is obtained by convolving the detector image or shadowgram with a decoding array derived from the spatial characteristics of the mask. For each sky image there is an intensity map (I), a variance map (V) proportional to the total counts recorded in each pixel, and a significance map (S) constructed from these as $S = I/\sqrt{V}$. Given that source photons are a very small fraction of the total counts, the background heavily dominates and the histogram of significance values for a given deconvolved image should follow the standard Normal distribution. Significant detections appear as spikes in the positive tail of the distribution. A broadening of this distribution is caused by systematic effects unaccounted for in the standard analysis software. Therefore, the standard deviation of the distribution of significance values can be effectively used to characterize and quantify the quality of a given sky image, and must be taken into account when calculating the true detection significance of a signal in that image [†]. For this reason, we have weighted each sky image according to the variance of its significance distribution to produce sky maps in seven energy bands from 20 to 400 keV; namely 20–30, 30–40, 40–56, 56–85, 85–120, 120–200, 200–400 keV, and to construct the spectrum of the   source IGR J17456–2901. We also performed the analysis of another energy band from 500 to 522 keV which yielded upper limits compatible with the Spi detection of the electron-positron 511 keV annihilation line reported in Knodlseder et al. (2005) (see § 4). The mosaics were made using the *pixel spread* option in the   4.2 imaging procedure which by projecting and distributing pixel values on the final mosaic pixel grid, preserves the symmetry of the point spread function (   ) and allows the most accurate source positioning.

Since the central source is too weak to be fitted with the in the imaging procedure performed on each pointing, the light curve was obtained by extracting the count rate at the source's pixel position from each reconstructed image.

3.2. *Source position determination*

The densely populated region around Sgr A* contains at least eight sources detected by Isgri within 1 degree of the   . Since

[†] The method used to account for systematic effects on a per-ScW basis described here is equivalent to deriving a correction factor to the theoretical statistical uncertainty and applying it to each pixel in the variance map. It follows that any test statistic such as Pearson's χ^2-test in which the variance of each data point is used to weigh the associated data value when testing for a deviation from the mean, should be used with the corrected variance values, i.e. the statistical variance multiplied by the variance of the distribution of significance values.

the standard   pipeline does not perform simultaneous fitting of several sources, we have used a custom fitting procedure to determine the best fit positions of the sources in the neighborhood of the   . Sub-images 40×40 pixels in size centered on the radio position of Sgr A* were extracted from the mosaics in the different energy bands and fitted using a model that included up to eight point-sources, each characterised by a 2D Gaussian approximation of the system point spread function and applied in the   software (Gros et al. 2003)

The width of the   was left as free global parameter (1 for all sources) because for mosaics, the width of the final cannot be predicted. The presence of close sources and possible confusion does not influence the result since a very strong point-like source (1E 1740.7–2942) dominates the images and this parameter is basically determined by the fit of this source. The procedure gives us the possibility to fix the position of some sources and also to set a flat background level to be fitted together with the point-sources. The residual map is inspected to verify that the fitting procedure is performed correctly.

Statistical errors at 90% confidence level on the fitted positions were derived from the measured source signal-to-noise ratios using the empirical law determined through a systematic study of well known sources (Gros et al. 2003). Although the empirical function of the source location accuracy in terms of the detection significance was determined using images reconstructed from single pointings, it was recently validated on mosaics as well. These tests were performed on isolated point-sources and since we are studying a region where the source density is unusually high, we present the results of our simultaneous fit for all the sources in the field to show that the offsets from the known positions are compatible with the empirical point-source location accuracy (   ).

3.3. *Spectral extraction*

The standard Isgri spectral extraction software works on the basis of a single pointing in the following manner. Using a list of sources, the procedure first calculates the pixel illumination factor; a model of the shadow of the mask cast on the detector plane by a given source. With this set of modeled shadowgrams, the software then attempts to fit the detector image by adjusting the relative intensity of each source either together with the background level simultaneously or by subtracting a background map normalized to the mean count rate beforehand. These procedures therefore estimate the maximum likelihood intensity of each source and in each pointing. However, a difficulty arises in the case of week sources (~mCrab) that require very long exposure times to acquire sufficient statistics to be detected. In such cases, and in particular when a large number of sources have to be modelled, the most efficient way to derive a spectrum is to build and clean sky images in the desired energy bands and then to extract in each the intensity and its associated variance at the pixel that corresponds to the source position, and to calculate the weighted mean count rate. As was described in the previous section, the variance at a given pixel must be corrected to take into account the systematic effects that grow additively with exposure time. In the case of IGR J17456–2901, the flux and variance values were taken at the pixel that corresponds to the sky coordinates R.A. = 266.4168, decl. = –29.0078 (J2000) in each sky map; the position of Sgr A*.

3.4. *X-ray spectrum*

The X-ray spectrum in the range 1–10 keV was extracted using 2004 *XMM-Newton* data from a circular region centered on the position of IGR J17456–2901 and with a radius of 8 arcmin-

utes. This radius was chosen to match the 13′ full width half max ( ) of the Ibis/Isgri instrument derived from the quadratric sum of the projected pixel (5′) and mask element (12′) sizes (Gros et al. 2003).

For a spectral extraction in which a large portion of the camera's field of view is used as a collecting surface, it is most suitable to use *XMM-Newton* background event files compiled from high latitude observations to construct a background spectrum. The procedure can be summarized as follows. Epic , Mos 1 and Mos 2 event files are filtered to exclude all non X-ray triggers using the event flag and pattern, after which a good time interval ( ) selection is performed to exclude periods of solar flaring activity. The selection criteria are based on the count rates in the high-energy bands, i.e.: 10–12 keV for Mos 1 and Mos 2, and 12–14 keV for . An interval of 100 s qualifies as a if it has less than 18 cts for both Mos cameras and 22 cts in the case of the camera. These strict selection criteria ensure that only the cleanest parts of the observation are used. The resulting filtered event files are used to make images in the high-energy bands in which a uniform distribution of events is expected under the assumption that energetic charged particles heavily dominate the instruments' respective spectra at these energies and that these fall uniformly on the telescope. If no point-sources are visible in these images, the ratios of the average count rate in the images to that of the background event file are used to scale the background spectra.

4. RESULTS

We now come to the results we have obtained on the morphology of the Galactic nuclear region and on IGR J17456–2901, which we tentatively associated with the supermassive black hole Sgr A* in Bélanger et al. (2004), and whose features we investigate more thoroughly in the present paper. We use three means of investigation to study the various characteristics of the source. The mosaic provides the fine positioning and general shape of the emission from the source and its close neighbours. The individual sky maps provide the elements needed for a variability study from kilosecond to month time scales and the average spectrum of the source can be used to constrain the nature of the emission. Section 4.1 begins with a presentation of the results obtained from the mosaic in the range 20–40 keV on the morphology of the emission from the central degrees. This is followed by a discussion of the changes in the emission's morphology as a function of energy by looking at the mosaics in the different energy bands up to 85 keV, and ends with our results on the electron-positron annihilation line at 511 keV. In § 4.2 we discuss the light curves and variability of the central source on different timescales, and in § 4.3 present the broad-band high-energy spectrum of the central arcmins of the Galaxy. Preliminary results on the with the X-ray monitor Jem-X are briefly discussed.

4.1. *Mosaics and spatial characteristics*

The mosaic shown in Figure 1 was constructed by summing 2174 sky images from individual pointings and amounts to an effective exposure time of 4.7×10^6 s at the position of Sgr A*. This Figure presents the highest signal-to-noise Ibis/Isgri 20–40 keV image of the yet published, showing an excess of more than 45 in siginificance from the direction of Sgr A*.

To model the observed morphology we have assumed that the emission is due to the sum of the known high-energy point-sources of the region that have been detected by *Integral* at least once. The main sources are 1E 1740.7–2942, KS 1741–293, 1A 1742–294, SLX 1744–299/300, 1E 1743.1–2853, IGR J17456–2901 and SAX J1747.0–2853. The respective positions of these sources were derived from a simultaneous fit of all 8 sources in the 20–40 keV mosaic. All positions were left as free parameters except for that of SAX J1747.0–2853 that was fixed. This source was quite active for the period refered to as Spring 2004 and thus contibutes to the emission near the but since its global contribution is weak and it cannot be clearly resolved from 1E 1743.1–2853 we must fix its position.

The result of the fitting procedure is well illustrated in Figure 2 where we see the mosaic (left), the model (middle), and the residual map after subtraction of the model from the sky map (right). We can see that the spatial distribution of the modeled image resembles very closely that of the mosaic, even if the residues hint at the presence of a non-uniform underlying emission that is not properly taken into account in the tested model. The fitted source positions are listed in Table 2 where we also report the signal-to-noise, the estimated error radius corresonding to the 90% confidence level and the offset with respect to the proposed counterpart.

We find that the position of IGR J17456–2901, detected at a signal-to-noise level of 45 in this energy band, is R.A. = $17^h45^m42^s.5$, decl. = $-28°59′28″$ (J2000) with an uncertainty of 0′.75. The reliability of the derived position for this excess is supported by the fact that all the other sources in the field are very well positioned. The brightest source, 1E 1740.7–2942, is well within its associated error radius. For 1A 1742–294, the reported offset is very close to the value of , while in the case of KS 1741–293 the best known coordinate position itself has an uncertainty of about 1′ (Sidoli & Mereghetti 1999). The source we labeled SLX 1744–299, is in fact a system composed of two known X-ray bursters located within ∼ 3′ of each other (Skinner et al. 1990; Pavlinsky et al. 1994; Sakano et al. 2002) and for this reason we do not expect the fit to yield a position within the for either one of the two sources, independently of the detection significance. 1E 1743.1–2853, a well known, bright X-ray source (Porquet et al. 2003a) is almost certainly contributing to the high-energy emission in the region. However, performing the simultaneous fit using a single source to model the emission from the region around this source gives a centroid offset by about 2′ from the *XMM-Newton* position known to arcsecond accuracy; a result that is not compatible with the expected error. Since, as mentioned above, we know of one source detected by Isgri that was active over the course of the first part of 2004, namely SAX J1747.0–2853, we included it and fixed its position. This yields a fitted position for 1E 1743.1–2853 that is well within the uncertainty derived from the source's detection significance. The position of IGR J17475–2822 was compared to the center of the Sgr B2 complex and discussed below.

IGR J17456–2901 is located at 1′.1 from the radio position of Sgr A* and 0′.9 from the center of Sgr A East. It is therefore compatible with either of these sources. Indeed, even if its associated positional uncertainty of 0′.75 is somewhat smaller than the offset, we expect this to be slightly overestimated when fitting multiple close sources (i.e. within the full width of the). For example, in the case of the known source 1A 1742–294, the measured offset can be 20–30% times larger than the . Morever we have found that the positions of 1E 1743.1–2853 and IGR J17456–2901 can change by 0′.3–0′.4 depending on the model adopted, and in some cases IGR J17456–2901 is positioned only 0′.6 from Sgr A*. For this reason we adopt a final error radius for the central source (and for 1E 1743.1–2853 that has a comparable signal-to-noise ratio) of 1′, about 30% larger than the value of 0′.75 derived
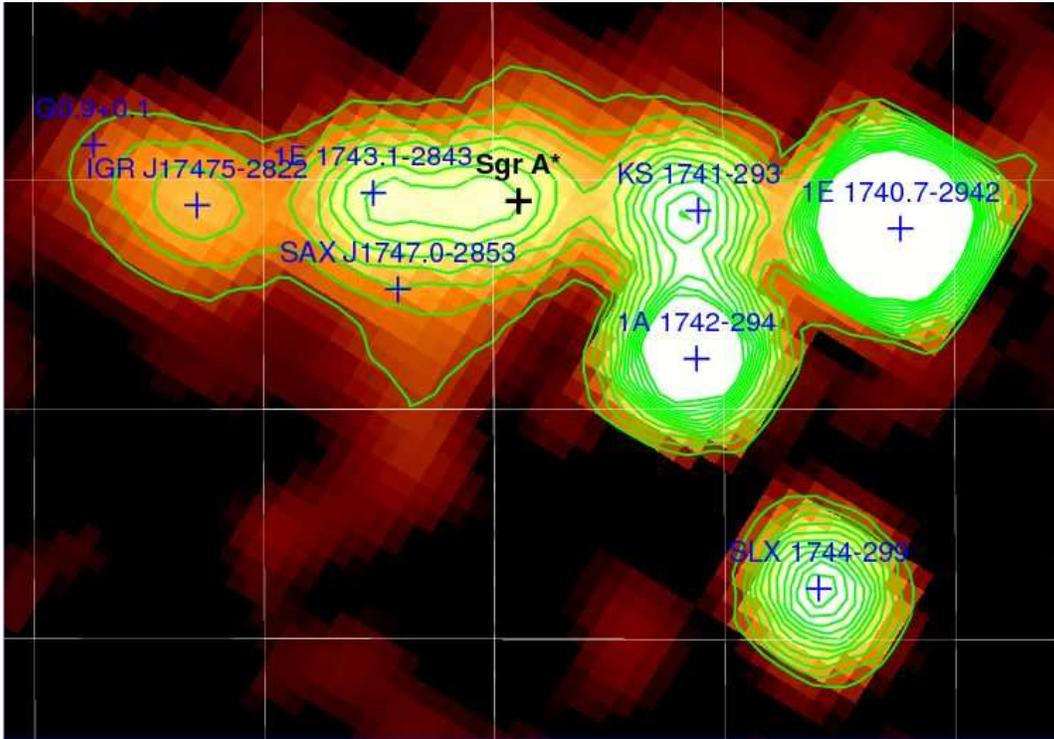
6

F .1.— Ibis/Isgri significance mosaic in the 20–40 keV energy range constructed from 2174 individual pointings with an effective exposure time at the position of Sgr A* of 4.7 Ms. Black indicates a statistical significance below or equal to 3 σ and white to a significance greater or equal to 60 σ. Contours mark iso-significance levels from 9.5 to 75 linearly. The orientation is in Galactic coordinates. The grid lines indicate galactic coordinates with a spacing of 0.5 degrees.
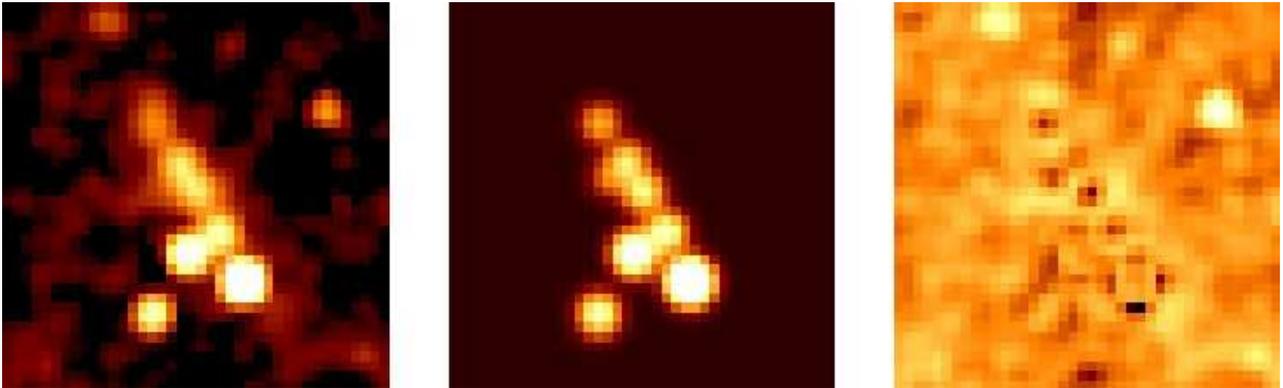

F .2.— Mosaic (left), model constructed from simultaneous fitting procedure of the 8 point-sources labeled in Figure 1 (center), and residuals after subtraction of model from mosaic (right). These maps are oriented in Equatorial coordinates where North is toward the top and East toward the left.

from the relation given by Gros et al. (2003).

On the other hand, we can safely exclude a number of other candidates such as the transient *Asca* source AX J1746.5–2901 (Sakano et al. 2002) mentioned by Revnivtsev et al. (2004) as a possible counterpart for the central excess based on the fact that it is located at a distance of more than 2′ from it.

A similar analysis was performed on the mosaics from the same data set in different energy bands. As is clearly seen from the iso-significance contours in Figure 3, the morphology of the central degrees does not radically change with increasing energy. However, we notice that the emission that seems to bridge the sources labelled Sgr A* and 1E 1743.1–2843 at low-energy persists at higher energies such that in the 56 to 85 keV range, the emission from the region seems to be centered between the two sources. This is a surprising result that we cannot readily

interpret. An investigation of this based on a comparison of the emission detected by Ibis/Isgri with the 20 cm radio map, the 6.4 keV Fe line-emission contours and the CS map of the region raises several other interesting questions.

Figure 4 is a radio continuum map at 20 cm (Yusef-Zadeh et al. 2004) on which we have overlayed the 20–30 keV iso-significance Isgri contours as they are shown in Figure 3 (top left). Firstly, the centroid of the very bright Sgr A complex which includes the luminous Sgr A East appears to be in best agreement with the 20–30 keV Isgri contours (Fig. 3 top left). For completeness, we performed the simultaneous fit using the position of Sgr A East instead of the one for Sgr A* and obtained very similar results. The offset of the fitted source is nonetheless slightly smaller for Sgr A East that for Sgr A* but both are within the   and

thus statistically equivalent. We also see that the radio Arc is quite distant from the peak near Sgr A* and can therefore be confidently excluded as a possible contributor to the flux at that position. However, the rough alignment of the radio Arc with the elongation on the 20–30 keV contours in the direction of negative latitudes is intriguing. In the 56–85 keV contours (Fig. 3 bottom right) we see that the centroid of the emission is almost exactly between the Sgr A complex and the radio Arc. This region is known to harbour large molecular clouds and there appears to be a very good agreement between this high-energy emission feature and both the 6.4 keV Fe line-emission, tracing irradiated molecular regions, and the CS map, tracing regions with high gas density. Furthermore, the centroid of this high-energy source is strikingly close to that of the unidentified *Egret* source 3EG J1746–2851 and could in fact be its soft γ-ray counterpart. We extracted a spectrum for this source by fitting three sources, two of which had their positions fixed to those of Sgr A* and 1E 1743.1–2853, and obtained a power-law photon index of $\Gamma \sim 2.3$, and a luminosity of $L_X[20–120 \text{ keV}] \sim 2.6 \times 10^{35}$ erg s^{-1} for a distance of 8 kpc. A more detailed analysis of this source will be presented in future work.

Moving in the direction of positive longitudes, we clearly see an emission region depicted in the 20–30 keV contours and whose centroid is labeled as IGR J17475–2822; a source associated with Sgr B2 by Revnivtsev et al. (2004). Indeed this source coincides with the radio-bright Sgr B2 complex composed of molecular clouds and several compact HII regions. The fitted centroid for this source, taken to be point-like in the 20–40 keV image, is positioned 1'.6 from the estimated center of the cloud. As was pointed out by Revnivtsev et al. (2004), there is good agreement between the 6.4 keV Fe line contours and the emission detected by Isgri as IGR J17475–2822. Moreover, the extension toward the north could tentatively be associated with the composite G 0.9+0.1 (Helfand & Becker 1987). The X-ray emission of its pulsar wind nebula (   ) has been mapped with *XMM-Newton* (Porquet et al. 2003) and the extrapolation of the flux towards 20 keV of about 9×10^{-5} ph cm^{-2} s^{-1}, is consistent with the residual flux of roughly 0.06 cts/s (20–40 keV) or 8×10^{-5} ph cm^{-2} s^{-1}. It is therefore tempting to interpret it as a detection of the highest energy synchrotron radiation from this source that was detected for the first time this year by the *Hess* instrument (Aharonian et al. 2005a). It is worth noting that a long *XMM-Newton* exposure of this object has revealed the presence of variable source probably of an accreting binary type, located at a distance of 1' (Sidoli et al. 2004). Having a luminosity close to that of G 0.9+0.1, its contribution to the residual Isgri emission could be significant.

We performed the analysis of the entire data subset used to construct the mosaics in the narrow band between 500 and 522 keV. This corresponds to the   of the emission line in the Isgri instrument (Terrier et al. 2003). A background map that corresponds to this energy range was used and thus the resulting mosaic is free of systematic effects. No sources are detected in the field spanning 10 degrees on either side of the   both in longitude and latitude. We obtain a 3σ upper limit of 1.9×10^{-4} ph cm^{-2} s^{-1} to the flux from a point-source at the position of Sgr A* where the exposure and thus the sensitivity is maximal. This limit is calculated taking into account corrections derived from the probability of photoelectric interaction at 511 keV in the Isgri detector (34%) and the fact that we have selected events using a band corresponding to 78% of line flux. Spi detected a 511 keV line flux of about 10^{-3} ph cm^{-2} s^{-1} with intrinsic line width of 2.7 keV (   )

TABLE 2

P	*Integral*	G		
Source ID	Signif.	Fitted position (R.A., decl.)	a (arcmin)	Offset[b] (arcmin)
1E 1740.7–2942 ..	241.8	265.9794, −29.7430	0.28	0.14
1A 1742–294	98.6	266.5138, −29.5109	0.40	0.55
SLX 1744–299 ...	61.8	266.8600, −30.0183	0.60	1.14
KS 1741–293	63.9	266.2130, −29.3327	0.59	1.23
1E 1743.1–2843 ..	46.3	266.5782, −28.7378	0.74	0.54
Sgr A*	45.4	266.4285, −28.9918	0.75	1.13
IGR J17475–2822.	18.9	266.8422, −28.4139	1.24	1.51
SAX J1747.0–2853	16.5	266.7500, −28.8700	1.45	0.0

[a]Point-source location accuracy at 90% confidence level
[b]Distance between the fitted and nominal source positions
[c]Position was fixed in the fit

from a region well described by a Gaussian with a   of about 8° and that coincides approximately with the Galactic bulge (Knödlseder et al. 2005). If we assume that our sensitivity is more or less uniform over the central 10 degrees around Sgr A*, our upper limit implies that if this emission is due to a collection of n point-sources clustered together such that they cannot be resolved by Spi, then under the simplifying assumption that they all contribute equally to the total flux, each must have a flux of about $\frac{1}{n} \times 10^{-3}$ ph cm^{-2} s^{-1}. Therefore, at least 5 individual sources would be necessary to account for this extended 511 keV emission in general agreement with the Spi result (Knödlseder et al. 2005).

Finally, Jem-X mosaics in four energy bands, with a total exposure is 3.2 Ms and effective exposure at the location of Sgr A* of about 500 ks, were constructed from 1204 science windows taken between 2003 February to 2004 October. We used the following energy ranges: 3–4, 4–8, 8–14, 14–35 keV and find no evidence in this data sample for the presence of a Jem-X source in the Sagittarius A complex except for a very marginal excess in the 8–14 keV mosaic. Although this analysis is preliminary and at this point somewhat qualitative, it is an interesting result in the light of the strong Isgri detection and obvious intense X-ray emission from this region seen by *XMM-Newton* and *Chandra*. It may be an additional indication that the emission is not due to a point-source but rather to a compact diffuse emission region were thermal and non-thermal processes take place.

4.2. *Light curves and variability study*

The complete light curve of IGR J17456–2901 in the 20–40 keV energy range, with a resolution of about 1800 s corresponding to the duration of a single pointing, is shown in Figure 5. Since low amplitude variability on kilosecond time scales can not be meaningfully studied for such a weak source due to statistical limitations, we have also done a search on longer time scales by rebinning the total light curve on the basis of 1 day, 2 weeks and 1 month. These rebinned data sets are presented in Figure 6.

No individual point deviates from the mean by more than 3σ. The level of variability in the flux from the central source was evaluated by means of a simple chi-squared test. For the unbinned data set shown in Figure 5, the reduced chi-squared value is $\chi^2_\nu = 1.3$ (2758/2093). For the light curve with 1-day time resolution (Fig. 6 top) we found $\chi^2_\nu = 1.7$ (180/109). In the case of the 2-week time resolution light curve (Fig. 6 middle), the reduced χ^2 value was found to be 3.6 (61/17). However, if we exclude the first point in this data set which corresponds to
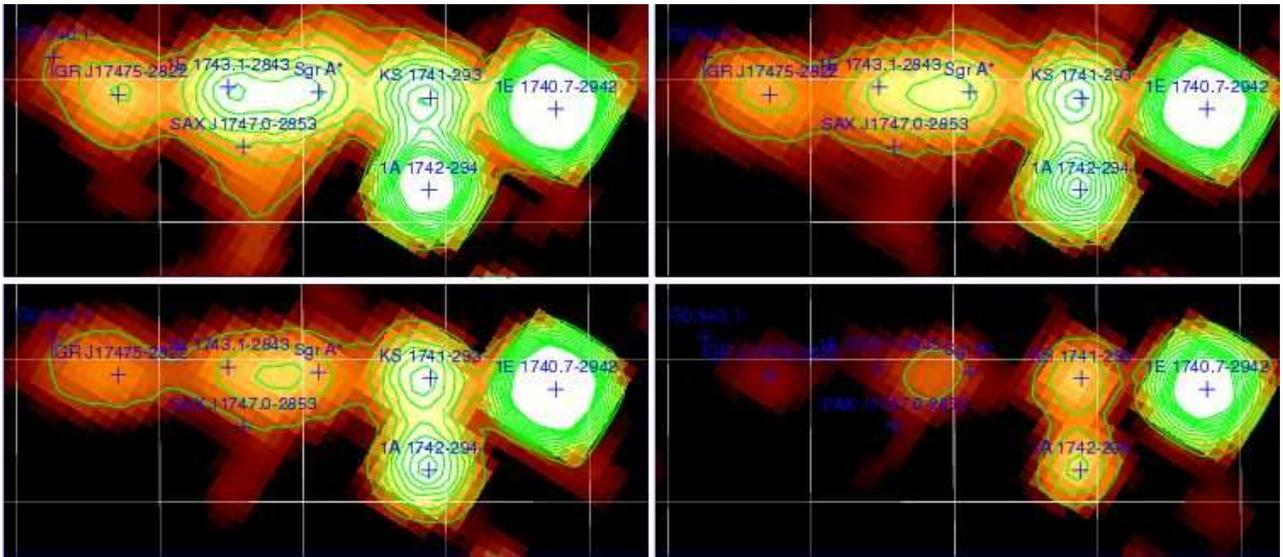
F .3.— Ibis/Isgri significance mosaic as in Figure 1 in four energy bands: 20–30 keV (top left), 30–40 keV (top right), 40–56 keV (bottom left) and 56–85 keV (bottom right). Black corresponds to statistical significance below or equal to 3 and white to a significance greater or equal to 50. The 12 contours levels mark iso-significance from 8 to 70 linearly.
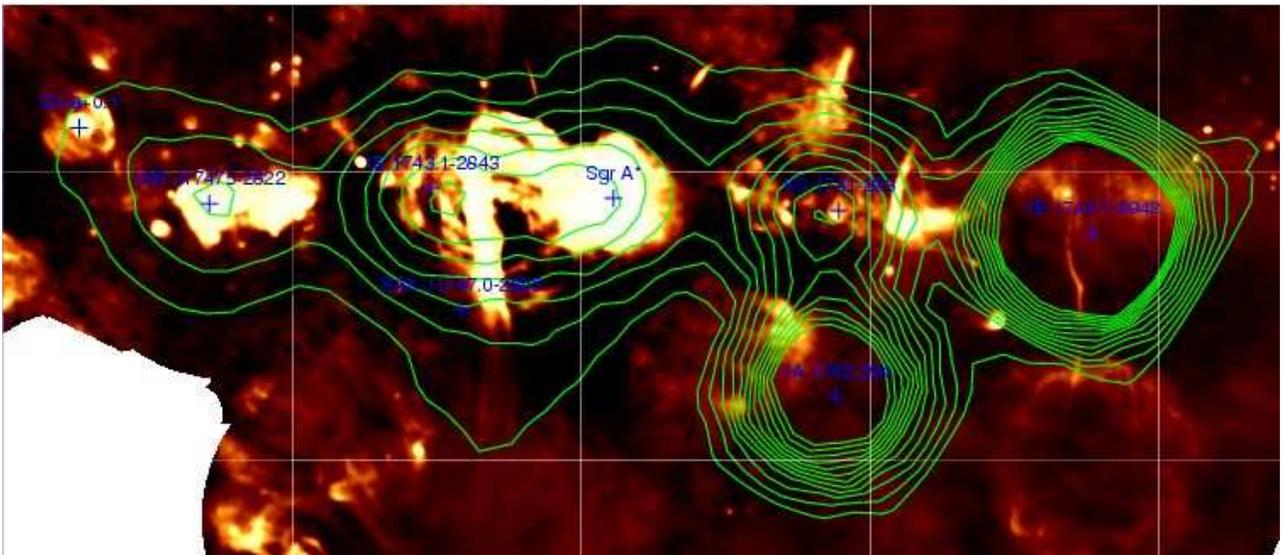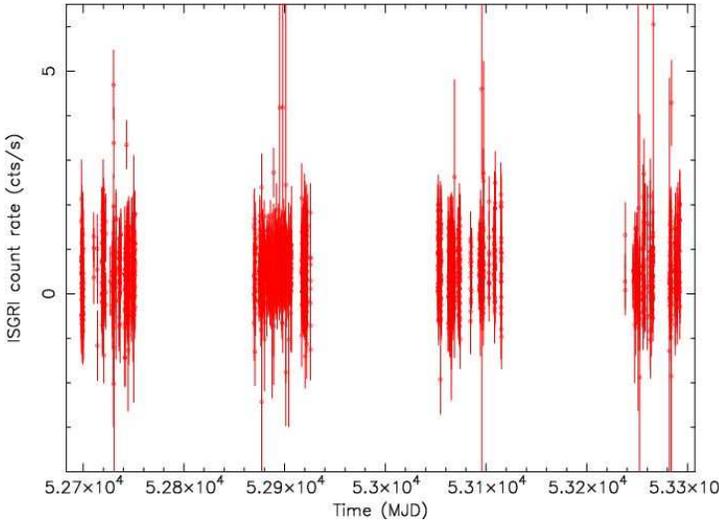

F .4.— Radio map of the Galactic center region at 20 cm overlayed with the 20–30 keV Isgri contours.

the data collected during revolution 46, the first observation of the just after the initial calibration phase, we find a value of $\chi_\nu^2 = 2.1$ (34/16), in closer agreement with the previous two. Finally, in the case of the 1-month time resolution light curve (Fig. 6 bottom) we find values of 5.2 (52/10) and 3.1 (28/9) if we exclude the first data point, heavily affected by the revolution 46 data given that there is a three-week gap between this revolution and the second observation of the during revolution 53. These reduced chi-squared values tend to increase as the binning gets coarser and thus we might be seeing a small level of variability on monthly timescales. Disregarding the data point associated with rev. 46, the only deviation that almost reaches 3σ from the mean is at the very end of the light curve where. This lack of evidence for significant variations in flux other than the low level of variability seen on monthly timescales is in contradiction with the previous detection of

a flare from IGR J17456–2901 (Bélanger et al. 2004) that we therefore do not confirm. We point out that those results were obtained with the preliminary analysis procedures and without background corrections. The data subset covering the observation period of the reported flare (2003 April) processed with the most recent analysis software and background correction maps do not indicate significant variability with respect to the mean count rate. Similarly, the sources 1E 1743.1–2843 and IGR J17475–2822 seem rather constant unlike the four well known X-ray binaries that show very large intensity variations over the two-year observation period.

4.3. Spectrum of IGR J17456–2901

Figure 7 shows the Isgri spectrum of the source that we modelled with a simple power-law of index $\Gamma = 3.04 \pm 0.08$ ($\chi^2 = 7.92$ for 5 dof and 3% systematics). The pegged power-law model *pegpwrlw* in Xspec uses the total flux as nor-
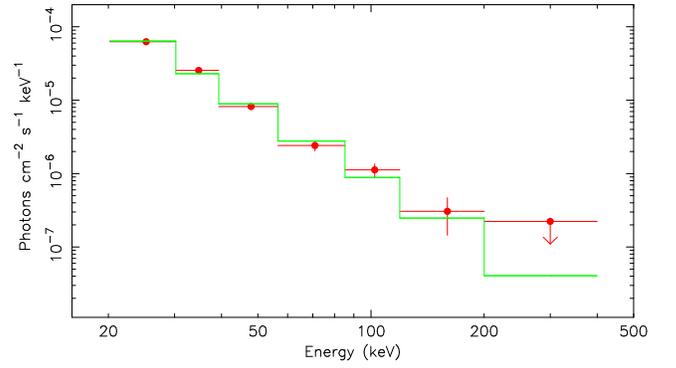
Fɪɢ. 7.— Two-year averaged Isgri spectrum of the source IGR J17456–2901 in the range 20–400 kev. The spectrum is fit with a power-law normalized over the whole energy range and yields a photon index of $\Gamma = 3.04 \pm 0.08$. Total flux is $(7.02 \pm 0.27) \times 10^{-11}$ erg cm^{-2} s^{-1}. The last point in the spectrum corresponding to the range 200–400 keV is given as the 1 σ upper limit, and the data point in the 120–200 keV band has a significance $\sim 2\,\sigma$

Fɪɢ. 5.— Light curve of IGR J17456–2901 in the 20–40 keV band constructed from 2174 sky images, each corresponding to one pointing (1800 s).
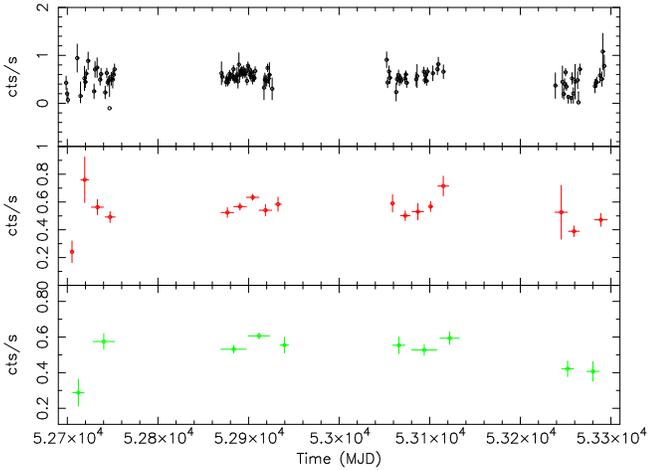
Fɪɢ. 6.— Rebinned light curves of IGR J17456–2901 constructed from the data set shown in Figure 5 with time bins of 1 day (top), 2 weeks (middle) and 1 month (bottom).

malization and in this way the photon index and normalization are independent paraters. The total flux in the range from 20 to 400 keV is $F_{X}[20–400\ \text{keV}] = (7.02 \pm 0.27) \times 10^{-11}$ erg cm^{-2} s^{-1}, which corresponds to a luminosity of $L_{X}[20–400\ \text{keV}] = (5.37 \pm 0.21) \times 10^{35}$ erg s^{-1} at a distance of 8 kpc to the . In the 20–100 keV range, the luminosity is $L_{X}[20–100\ \text{keV}] = (4.56 \pm 0.10) \times 10^{35}$ erg s^{-1}, somewhat higher than our first estimate of $\sim 3 \times 10^{35}$ erg s^{-1} (Bélanger et al. 2004). This is not surprising given that the first estimate was based on a rough comparison with the Crab's count rate in only two energy bands, 20–40 and 40–100 keV, and that we now have 5 points to constrain the slope. Furthermore, the detection significance of the central source was much lower than in the present case.

Now turning to the broad-band high-energy spectrum of IGR J17456–2901, we can see in Figure 8, the spectrum of the central source from 1 to 400 keV where the X-ray portion (1–10 keV) is from *XMM-Newton* data collected during the multiwavelength campaign, and therefore contemporaneous with part of the Isgri data from 2004 used to construct the soft γ-

ray portion (20–400 keV) of the spectrum that was discussed earlier and is shown by itself in Figure 7. The X-ray spectrum was made by extracting the photon flux from a region centered at the position of IGR J17456–2901 and with an radius of 8′. This integration radius was chosen to be compatible with the Ibis/Isgri psf because there is no obvious X-ray point-source counterpart to IGR J17456–2901 within 1′ of Sgr A*. Such a point-source would have to be hard, persistant and extremely bright in X-ray in order to be compatible with the high-energy flux of the *Integral* source.

The model fitting for large extended regions near the is challenging for two main reasons. First, the X-ray spectra of such extended regions give a corse, averaged spectral behaviour of a complex field heavily dominated by diffuse emisson that we know to have several different spectral components (Muno et al. 2004a) but that also includes all the point sources some of which surely contribute to the hard X-ray flux. Of course, this difficulty dissipates as integration radius decreases since fewer components are summed together. Second, we have no *a priori* knowledge of the nature of the emission detected as IGR J17456–2901 and therefore do not know whether the comparison with the total X-ray spectrum from a region that roughly corresponds to Isgri's angular resolution is an appropriate one. Keeping these caveats in mind, we justify this type of comparison by pointing to the fact that the source coincident with the , detected by *Integral* as what appears to be a point-source, must undoubtedly contribute to the X-ray spectrum from the region that corresponds to its spatial extent. The spectral transition from 10 to 20 keV must be more or less continuous and therefore we expect the high-energy component present in the X-ray spectrum and from which IGR J17456–2901 arises, to stand out beyond the thermally dominated spectrum at around 20 keV. Therefore, a large χ^2 value should not be surprising for it points to the fact that the emission in the range from 1 to 3 keV is not modelled properly for the reason mentioned above. Our aims in this section is to constrain the high-energy characteristics of this source in the range 1–400 keV using the Isgri spectrum above 20 keV.

The broad-band spectrum can be modelled using a simple broken power-law over the entire range to get an idea of the change of spectral index with increasing energy. However, in order to be as constraining as possible without overlooking possibly important components to this emssion like the hot temperature plasma present in the region, we performed the fit with

TABLE 3

S M G C S

IGR J17456–2901

Quantity	Cutoff PL	Broken PL
$N_{H,1}$ ($10^{22}\,cm^{-2}$)	$7.81^{+0.02}_{-0.04}$	$7.79^{+0.11}_{-0.13}$
kT_1 (keV)	$1.002^{+0.008}_{-0.004}$	$0.99^{+0.02}_{-0.02}$
N_{kT_2}	$0.378^{+0.009}_{-0.006}$	$0.38^{+0.02}_{-0.02}$
$N_{H,2}$ ($10^{22}\,cm^{-2}$)	$13.13^{+0.17}_{-0.23}$	$13.52^{+0.56}_{-0.50}$
kT_2 (keV)	$6.56^{+0.07}_{-0.09}$	$6.60^{+0.13}_{-0.12}$
N_{kT_2} (10^{-2})	$6.35^{+0.05}_{-0.06}$	$6.45^{+0.01}_{-0.02}$
Γ_1	$1.09^{+0.03}_{-0.05}$	$1.51^{+0.06}_{-0.09}$
$E_{cutoff/break}$ (keV)	$24.38^{+0.55}_{-0.76}$	$27.13^{+2.79}_{-4.39}$
Γ_2	...	$3.22^{+0.34}_{-0.30}$
N_{Γ} (10^{-3} ph cm^{-2} s^{-1} keV^{-1})	$4.46^{+0.29}_{-0.27}$	$7.445^{+0.001}_{-0.001}$
χ^2 (dof)	4490.7 (2658)	4458.0 (2657)

Uncertainties on the parameters correspond to the 90% confidence level

the same model as the one used by Muno et al. (2004a) to fit the diffuse emission from the various regions in the $17' \times 17'$ field around Sgr A* referred to as Southeast, Southwest, Northwest, East, Close, and Northeast by the authors. This model comprises a two-temperature plasma with different absorption columns, a power-law and a gaussian line to fit the 6.4 keV neutral Fe emission line absorbed with the same column density. Although providing a reasonable fit to the data from 2–8 keV, the model does not work well in the Isgri range of the spectrum. The power-law fit with index $\Gamma \approx 2$ underestimates the flux in the 20–40 keV range and overestimates it above 85 keV. A somewhat better fit is provided by replacing the simple power-law with either a cutoff or broken power-law. In the case of the cutoff power-law, we found a photon index $\Gamma \approx 1$ and cutoff energy of about 25 keV, and in the case of the broken power-law, the photon indeces were found to be $\Gamma_1 \approx 1.5$ and $\Gamma_2 \approx 3.2$ with a break energy of about 27 keV. The best fit parameters values are given in Table 3 where only the free parameters are listed; all abundances are fixed to solar abundance.

Looking closely at the unfolded spectra shown in Figure 8, we can distinguish the low and high temperature plasma components drawn in red and green respectively, the gaussian line in light blue and the broken power-law in dark blue. The hot thermal component clearly dominates the spectrum at low-energies but its contribution is already well below that of the power-law component in the 20–30 keV band and is totally negligible beyond that. If we fix the temperature of the hot component at 8 keV, the effect on the other parameters is small. The photon index in the cutoff power-law decreases from 1.09 to 1.05 and the high-energy cutoff from 24.4 to 27.7 keV. The χ^2 value increases to 4849.0 for one more dof and therefore the reduced chi-squared is slightly larger i.e. $\chi^2_\nu = 1.82$, and the contribution of this component to the overall flux in the 20–30 and 30–40 keV bands increases by a factor of 2 but still lies 3 times below the power-law in the first band and a factor of 7 below in the second.

4.4. Multiwavelength campaign

A multi-wavelength campaign to study Sgr A* with a total exposure time of about 500 ks was performed in two segments, the first of which was from 2004 March 28 to April 1 and that we refer to as epoch 1, and the second from 2004 August 31 to September 3 refered to as epoch 2. The primary aim of this campaign was to study correlated variability, particularly in the IR, X-ray and soft γ-ray energy bands. Figures 9 and 10 show the 2–10 keV *XMM-Newton* light curve of a 10″ region around Sgr A* in the bottom panels, and the 20–30 keV Isgri light curve of IGR J17456–2901 in the upper panels for epochs 1 and 2 respectively. As is clearly visible, the periods during which the factor-40 flares from the direction of Sgr A* occured do not have simultaneous coverage in the *Integral* data. Unfortunately, both data gaps in the Isgri light curve correspond to the period between orbits. For this reason we are still unable to conclude whether or not we can expect to detect a correlated variability in the X-ray and soft γ-ray bands. There are two features worth mentioning that can be noticed in Figure 10 although they have marginal statistical significance. First, two points in the Isgri light curve, approximately in the middle of the upper panel, stand out at about $2.5\,\sigma$ above the mean. These are temporally coincident with the two hiccups at the end of the first data subset in the X-ray light curve shown in the bottom panel. Second, the weighted mean X-ray count rate is somewhat higher in the first data subset (0.30 ± 0.001 cts/s) than in the second (0.27 ± 0.001 cts/s), a behaviour apparently seen also in the two corresponding segments of the Isgri light curve where the weighted mean count rate is 0.42 ± 0.03 cts/s in the first and 0.20 ± 0.07 cts/s in the second. This indicates that there may be a relationship between the flaring activity of Sgr A* and emission at higher energies. Future simultaneous observations will undoubtedly help elucidate this point which remains uncertain.

5. SUMMARY AND DISCUSSION

5.1. Summary

We have studied the morphology of the high-energy emission from the central few degrees of the Galaxy in the energy range from 20 to 400 keV based on a sample of *Integral* data collected from 2003 February to 2004 October with a total live-time of 7×10^6 s. We paid particular attention to the characteristics of the emission from the Galactic nuclear region where we detect a source with high significance in the 20–40 keV energy range located at R.A. = $17^h45^m42^s.5$, decl. = $-28°59'28''$ (J2000) with an uncertainty of 1′ and therefore compatible with the position of the central black hole Sgr A*. This detection confirms the results obtained by Bélanger et al. (2004) on the source IGR J17456–2901.

The source IGR J17456–2901 is persistent and shows no variability at the 3σ level in contradiction with what was suggested to in Bélanger et al. (2004). This result holds at kilosecond, daily, bi-weekly and monthly timescales.

The spectrum of the central source in the 20–400 keV range is well fit by a power-law of index $\Gamma \approx 3$. We have combined this dataset with the X-ray spectrum of a circular region with radius 8′ centered the *Integral* source derived from partially contemporaneous *XMM-Newton* data collected during observations of the performed in 2004 in the range 1–10 keV. From this we find that the broad-band high-energy spectrum can be fit equally well with a model that comprises a two-temperature plasma ($kT_1 \approx 1.0$, $kT_2 \approx 6.5$), a Gaussian line to account for the neutral Fe emission at 6.4 keV, and either a cutoff power-law with photon index $\Gamma \approx 1$ and cutoff energy of about 25 keV or a broken power-law with photon indeces $\Gamma_1 \approx 1.5$ and $\Gamma_2 \approx 3.2$, and break energy ≈ 27 keV.

We also detect hard ($\Gamma \sim 2.2$) emission from a region located between Sgr A* and the radio Arc that seems to coincides with the 6.4 keV emission from neutral to weakly ionised Fe and with the CS map of the region. As is the case with IGR 17475–2822, we believe that this new detection of hard X-ray emission orginates in one or several large molecular clouds known to exist in that region.
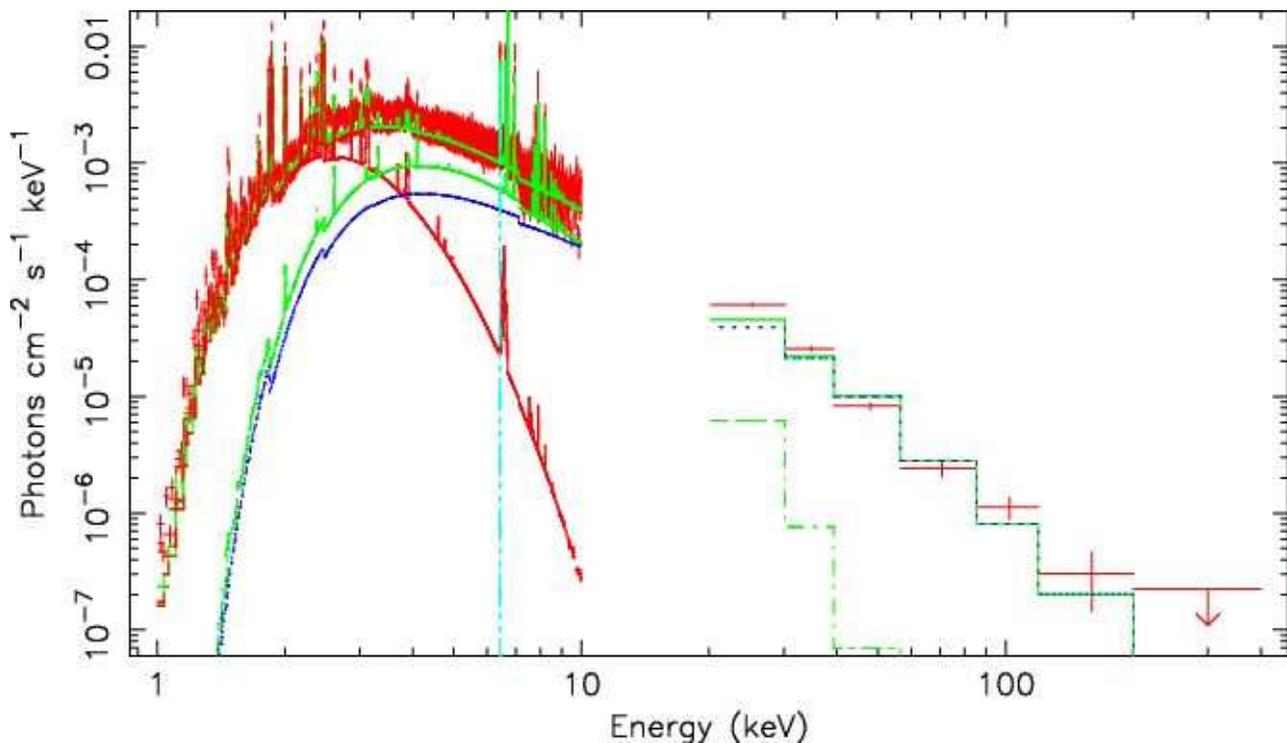
The nature of the emission from the direction of the Sgr A

F . 8.— Broad band high-energy spectrum of IGR J17456–2901 constructed from XMM-Newton data in the 1–10 keV energy range and from Isgri data from 20 to 400 keV. The X-ray portion of the spectrum was build by integrating over a circular region of radius 8′. The model used is an absorbed two-temperature plasma plus a broken power-law where the low and high temperature components are drawn in red and green respectively, the power-law is in dark blue and the 6.4 keV gaussian line is in light blue. As in Figure 7, the point in the last bin gives the 1 σ upper limit on the flux in the 200-400 keV range.
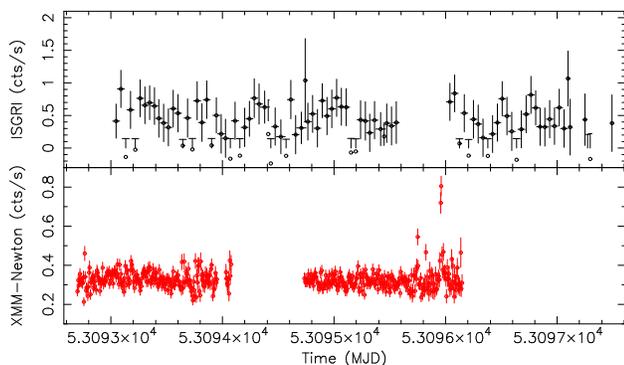

F . 9.— *XMM-Newton* light curve of the region within 10″ of Sgr A* in the 2–10 keV range with a time resolution of 500 s (bottom) and Isgri light curve of IGR J17456–2901 in the range 20–30 keV (top) with time resolution of about 1800 s for epoch 1 of the multiwavelength campaign. The data gaps correspond to the time between orbits for which there is no scientific data.
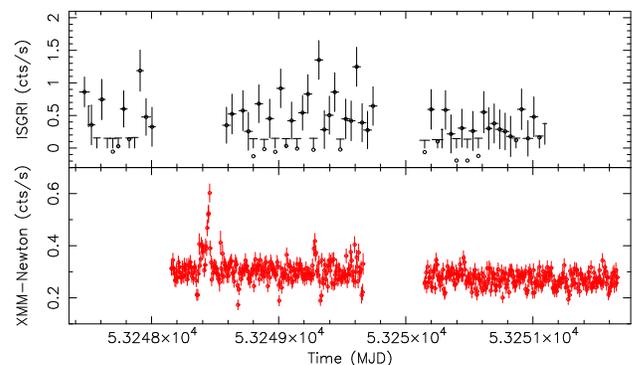

F . 10.— Same as in Figure 9 for observation epoch 2. The clear periodic dips in the *XMM-Newton* light curve are caused by the eclipses of the transient CXOGC J174540.0–290031 (Porquet et al. 2005b; Muno et al. 2005b).

complex detected as IGR J17456–2901 is unknown. In what follows we discuss a number of scenarios in an attempt to identify the source of the emission detected by *Integral* and apparently centered on Sgr A*.

5.2. *Hot plasma*

The hot component at 6–8 keV of the two-temperature plasma at the is well known and its presence is viewed by many as problematic in terms of it being confined given the escape velocity of a Hydrogen plasma at that temperature or of the heating mechanisms that would be required to supply energy to the plasma were it not confined. It is interesting to ask what is this hot plasma's extrapolated flux at energies between

20–30 keV in order to assess its possible contribution to the flux detected from the central arcminutes. In § 4.3 we showed that although the hot plasma component totally dominates the spectrum in the range from 2 to 5 keV, its contribution to the overall flux is several times less than that of the power-law in the 20–30 keV range and drops to a negligible level with respect to the power-law component in the range 30–40 keV. These estimates are based on the best fit value for the temperature of 6.5 keV and clearly the contribution increases somewhat if we fix the temperature at 8 keV. Nonetheless this hot plasma can only provide a very small fraction of the emission detected from the direction of the by *Integral*, and this solely in the first band, from 20 to 30 keV.

5.3. *X-ray transient sources*

A large number of X-ray transients have been detected in the neighbourhood of Sgr A* in the last few years (Muno et al. 2004b; Porquet et al. 2005a). In fact, there even appears to be an over-abundance of such sources near the where four X-ray binaries lie within 1 pc (25″) of Sgr A* (Muno et al. 2005a). These sources, observed at luminosities between 10^{33} and 10^{36} erg s^{-1} in the 2–10 keV range, are not particularly bright since these luminosities are intermediate between quiescence and outburst. In the paragraphs that follow we attempt to estimate the effect of such sources on the flux of IGR J17456–2901 in the 20–120 keV range. We restrict ourselves to this energy range because it is here that we have the best estimate of flux from the Isgri data.

The source IGR J17456–2901 shows very little variability and hence its persistant quality demonstrates that it is probably not heavily influenced by the sometimes radical brightening of an individual X-ray transient as it moves from quiesence to outburst. Furthermore, the high detection significance in the 20–40 keV band permits an accurate determination of the emission centroid and yields an uncertainty of about 1′. For this reason, we do not consider transients that lie outside the error radius of IGR J17456–2901 but turn our investigation to the 4 transients detected by *Chandra* within 30″ of the central (Muno et al. 2005a) and pay particular attention to the remarkable located just 3″ south of Sgr A* (Muno et al. 2005b). This transient, CXOGC J174540.0–290031, was very bright during both epochs of the multiwavelength campaign, the only period for which we have contemporaneous X-ray and *Integral* data, and will therefore be the main focus of the discussion.

The four transients detected within 30″ of Sgr A* are also the hardest of the seven transients discussed by Muno et al. (2005a). These are: CXOGC J174535.5–290124, CXOGC J174538.0–290022, CXOGC J174540.0–290005 and CXOGC J174540.0-290031. Using the available *Chandra* data for these (and *XMM-Newton* for CXOGC J174540.0–290031), we constructed their respective light curves in the range 2–8 keV and rebinned to make the long term trends more apparent (the *Chandra* results were published in Muno et al. (2005a)). We plotted the light curve for IGR J17456–2901 rebinned in 2 week segments on the same time line. The 20–40 keV range is used because it has the highest signal-to-noise ratio. Figure 11 shows these light curves where that of IGR J17456–2901 appears as the top most. The flux is in units of ph cm^{-2} s^{-1} and the time is in modified Julian days.

The observation cycles are clearly depicted by the Isgri light curve where each data subset corresponds to a season, the first one being Spring 2003 and the last, Fall 2004. As was found in § 4.2, there is no clear sign of variability in the *Integral* light curve other than the close to 3σ deviation in the very last part of the light curve. Furthermore, it is difficult to draw conclusions from the general comparison with the flux levels of the four hardest *Chandra* transients shown in Figure 11. We will now take a closer look at the unusual transient CXOGC J174540.0–290031.

This source was discovered during the 2004 July *Chandra* observations of the (Muno et al. 2005b) and was also seen to be active throughout both epochs of the multiwavelenth campaign of 2004, reaching its peak X-ray brightness in April. A very clear periodic signal was detected from this source during epoch 2 and the orbital period was determined to be about 8 h (Porquet et al. 2005b; Muno et al. 2005a; Bélanger et al. 2005). This source, located remarkably close to the supermassive at only ∼ 3″ from the radio position of Sgr A*, was observed in radio during the campaign
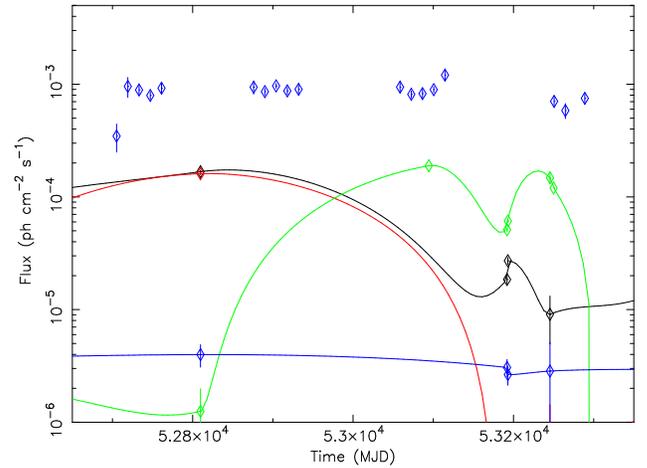

F . 11.— Light curves in the 2–8 keV energy range of CX-OGC J174535.5-290124 (black), CXOGC J174540.0-290005 (red), CX-OGC J174540.0–290031 (green), CXOGC J174538.0-290022 (blue) and in the 20–40 keV range for IGR J17456–2901 binnned in 2-week periods.

(Bower et al. 2005), and seen to produce a jet with luminosity $L_{jet} \sim 10^{37}$ erg s^{-1}.

In order to estimate the possible contribution of this source to the *Integral* flux, we used the spectral parameters derived from the contemporaneous *XMM-Newton* observations and presented in Porquet et al. 2005. Taking a photon index of $\Gamma = 1.6$ and 2–10 keV flux normalization of 1.3×10^{-12} erg cm^{-2} s^{-1} we find that the extrapolated 20–120 keV luminosity is about 5×10^{34} erg s^{-1}. For an index $\Gamma = 1.98$ and flux $F_X = 1.8 \times 10^{-12}$ erg cm^{-2} s^{-1}, we get an extrapolated luminosity of 2.5×10^{34} erg s^{-1}. The largest of these values amounts to about one tenth of the derived luminosity of IGR J17456–2901 and is probably still over-estimated given that the spectrum of a in outburst is rarely a pure power-law above energies ∼ 100 keV. A more realistic description would be a comptonization model where the seed photons are boosted to higher energies as they encounter fast thermal electrons in the hot (30–50 keV) corona. In this case, the contribution in the Isgri band would very likely be even less than the above extrapolations. According to this simple estimate, ten sources similar to CXOGC J174540.0–290031 in luminosity and spectral index within a few arcminutes of Sgr A* would have to be active more or less continuously to account for the 20–120 luminosity of IGR J17456–2901. Of course, the flux could be due to a substantially larger number of dim and hard sources that have until now evaded detection by *Chandra* and *XMM-Newton* and that are clustered around Sgr A*. This however, is an unlikely scenario.

We have considered and tried to quantify the effect of the known X-ray transients located within 30″ of Sgr A* on the Isgri count rate. We find that the flux of IGR J17456–2901 can not be explained by the contribution of transients located very close to the central , and that their contribution appears to be negligeable over the range from 20 to 120 keV.

5.4. *Flares from Sgr A**

Our campaign to search for correlated variability in the X-ray and soft γ-ray flux from the central was inconclusive due to *Integral* data gaps during the Sgr A* flares. Of the two factor-40 flares that occured on 2004 March 31 and August 31, the first was somewhat harder with a photon index of $\Gamma = 1.52$ compared to $\Gamma = 1.87$ for the second flare (Bélanger et al. 2005). By

extrapolating the flux of the hardest flare to the 20–30 keV energy band we find that its contribution to the Isgri count rate using an average effective area in this band of 650 cm^2 should be about 0.05 cts/s. Taking a peak flare flux equivalent to twice the average gives 0.1 cts/s and so since IGR J17456–2901's observed Isgri count rate in this range is around 0.4 cts/s we would expect a rise of $\sim 25\%$ due to the flare. Based on these simple assumptions, this type of event would therefore not be detectable by Isgri, and for the same reason, cannot explain the emission seen as IGR J17456–2901.

Furthermore, the derived luminosity of the source of around 5×10^{35} erg s^{-1}, cannot result directly from the integration of successive flares from the central black hole. The flares occur on average once per day and have typical luminosities of 10^{35} erg s^{-1} for durations of a few thousand seconds. If the flares last 3 to 20 ks, even if they all reached peak luminosities of around 10^{36} erg s^{-1}, this would still not be enough to make up the persistant luminosity of IGR J17456–2901. This is not to say, that the acceleration of particles to very high lorentz factors during such a flare could not lead to a secondary high-energy emission that would not be detected by X-ray instruments but that would contribute to the flux in the range 20–400 keV.

5.5. *Charged particle acceleration*

The detection of a persistant source up to about 120 keV compatible with the position of the central raises the very interesting possibility that it may be related to the TeV source detected from the same region by *Hess* (Aharonian et al. 2004). These observations lend crucial support to the idea that acceleration of particles to very high energies is taking place at the (Crocker et al. 2005). Furthermore, all of them agree on the apparent absence of variability from the central source.

The *Hess* Collaboration has been particularly successful at determining the high-energy properties of this source detected over two epochs, 2003 June-July and 2003 July-August, and together with the earlier 30 MeV to 10 GeV *Egret* detection of the continuum source 3EG J1746–2851 within 1° of the nucleus (Mayer-Hasselwander et al. 1998), this TeV detection provides some evidence of hadronic acceleration at the , either by Sgr A* itself, within the shocked shell of an , such as Sgr A East or by some other mechanism inlcuding the interaction of non-thermal filaments with dense molecular environments. Protons could be accelerated, either via 1st order Fermi acceleration at a shock, or via stochastic acceleration (a 2nd order Fermi process) in a turbulent magnetic field, and then scatter with ambient protons to produce pions. The π^0's subsequently decay into 2γ-rays, whereas the π^+'s and π^-'s initiate a muon, electron, positron, and neutrino cascade (see e.g., Markoff, Melia & Sarcevic 1997,1999). Some evidence for a pion origin of the γ-rays is provided directly by the *Egret* spectrum, which exhibits a clear break at ~ 1 GeV, and therefore cannot be fit by a single power law. Instead, this break is usually attributed to the rest-frame energy of pion-decay photons. The secondary electrons and positrons produced by the charged pions in concert with the π^0-decay photons, are capable of producing their own γ-ray emission via bremsstrahlung and Compton scattering. For example, if these leptons build up to a steady-state distribution balanced by bremsstrahlung and Coulomb losses, they naturally account for the lowest energy *Egret* datum. This is rather important because the pion decays link the lepton and photon generation rates, so the bremsstrahlung and pion-decay photon emissivities are tightly correlated.

The possibility that the relativistic protons may be accelerated close to Sgr A* was first explored by Markoff, Melia &

Sarcevic (1997, 1999), who concluded that the maximum attainable energy is of the order of 4×10^5 TeV. However, there appear to be two principal reasons why the pp scatterings that lead to pionic γ-ray emission probably do not occur in the acceleration zone itself. First, the ensuing particle cascade would produce a copious supply of energetic leptons that, in the presence of the inferred ~ 1–10 G magnetic field for this source, would greatly exceed Sgr A*'s observed radio flux. Second, the lack of variability in the data from keV to TeV energies, argues against a compact point-source like Sgr A*. The more recent analysis of proton acceleration within Sgr A* (Liu, Petrosian & Melia 2004; Liu, Melia & Petrosian 2005) has shown that these relativistic particles actually diffuse to distances ~ 2–3 pc away from the acceleration site before scattering with the ambient protons, and therefore the ensuing leptonic cascade does not overproduce emission at longer wavelengths having left the region where the magnetic fields are very strong. In support of this picture, wherein the relativistic particles responsible for the *Hess* and *Integral* source are accelerated near Sgr A*, it is worth noting that the mechanism responsible for accelerating the electrons required to account for Sgr A*'s 7 mm emissivity, also accelerates protons in the system. These protons do not radiate as efficiently as electrons and therefore diffuse away from the acceleration site. The electron acceleration rate implied by the radio measurements also corresponds to the right $\sim$ TeV luminosity from the protons flooding the region surrounding the black hole to match the *Hess* measurements. In addition, the time required for these particles to diffuse outwards is $\sim 10^5$–10^6 years, which would argue against any rapid variability in the TeV γ-ray emission, as observed. Thus, although both the *Hess* and *Integral* sources appear to be slightly extended, the origin of the particles responsible for the broad band spectrum of the nuclear region may ultimately still be Sgr A*.

5.6. *Sgr A East*

The supernova renmant Sgr A East whose centroid is located 50″ from Sgr A*, is another likely source of γ-rays near the (see Melia & Falcke 2001). It is a member of a class of remnants detected at 1720 MHz (the transition of OH maser emission), a signature of shocks produced at the interface between supersonic outflow and the dense molecular cloud environments with which they interact. It has already been shown (Fatuzzo & Melia 2003) that Sgr A East is capable of producing the observed γ-ray luminosity detected by *Egret* once the unusually-high ambient particle density ($> 10^3$ cm^{-3}) and strong magnetic field (> 0.1–0.2 mG) are taken into account. In a thorough examination of the particle acceleration and energetics in this source, Crocker et al. (2005) demonstrated that Sgr A East could very well also be the source of the TeV spectrum measured by *Hess*. One should note, however, that the *Egret* and *Hess* sources are probably not coincident. The centroid of the *Egret* emission (Mayer-Hasselwander et al. 1998) appears to be significantly displaced away from Sgr A*, whereas the TeV source lies within $\sim 1'$. In addition, although the *Egret* and *Hess* spectral indices are similar (~ 2.2), the corresponding fluxes at GeV and TeV energies differ by over an order of magnitude. It appears that the *Egret* source must cutoff well below the TeV range suggesting, together with the relative spatial displacement of the two sources, that we must be dealing with at least two separate regions of γ-ray emissivity.

Sgr A East may in fact be a very good candidate as the source of the emission detected by *Integral* and *Hess* at the Galactic center. This composite in its radiative phase has several observational characteristics akin to supernovae in molec-

ular clouds or dense environments: a bright radio shell with a strong non-thermal synchrotron component, X-ray emission from the compact central core dominated by the hot thermal plasma component and a strong He-like 6.7 keV Fe emission line. It shares some of these features with G 0.9+0.1 that was recently confirmed as a source of TeV radiation by the *Hess* collaboration (Aharonian et al. 2005a) and its local environment make it a good candidate for powerful particle acceleration. There is one important distinction between G 0.9+0.1 and Sgr A East however; the compact core of G 0.9+0.1 is known to be a   for which is central pulsar has been detected (Gaensler et al. 2001) and that has a hard, non-thermal X-ray emission. The X-ray core of Sgr A East is so highly dominated by thermal emission that non-thermal X-ray emission does not even seem to be present. We know however, that such behaviour is not unexpected for   in molecular clouds or dense environments (Bykov 2002). Moreover, there is preliminary evidence that several of the new *Hess* sources detected during the Galactic plane scan might be   with weak X-ray emission (Aharonian et al. 2005b).

5.7. *Final comments*

The Isgri instrument on the *Integral* satellite has detected with a high significance hard X-ray and soft γ-ray emission centered within 1′ of the Galactic nucleus. We have analyzed two years of *Integral* observations and thoroughly examined this data over the energy range from 20 to 400 keV. Combining these results with *XMM-Newton* data in the energy range from 1 to 10 keV, we have found that this emission cannot be attributed to the hot thermal plasma in the Sagittarius complex, it cannot be explained by the integrated flux from known X-ray transients near the central black hole, and it cannot be the simple extrapolation of the X-ray flux of flares from Sgr A*. The fact that IGR J17456–2901 is comparable in brightness to the well known binary system 1E 1743.1–2853 in the 20–40 keV range but that unlike this source it does not produce the large X-ray flux that makes 1E 1743.1–2853 so incredibly conspicuous in the soft X-ray band suggests that IGR J17456–2901 is not point-like. In addition, the fact that Jem-X, with its ~ 3′ angular resolution, easily detects the known binaries in the re-

gion including 1E 1743.1–2853 but does not see any emission from the   also suggests that the nature of IGR J17456–2901 is not point-like. These considerations lead us to conclude that IGR J17456–2901 is a compact diffuse emission region a few arcminutes in size and where astrophysical processes give rise to thermal and non-thermal emission.

The power of investigation and discovery at our disposal through combining the use of very high resolution X-ray instruments like *XMM-Newton* and *Chandra*, radio observatories like the   , and the new generation of γ-ray telescopes like *Integral* and *Hess* at the highest energies is astounding. To be faced with data from observations that cannot be readily explained nor understood is stimulating and inspiring. This is the kind of puzzle that we face in trying to understand the nature of the emission detected from the direction of the Galactic nucleus with *Integral* and *Hess*.

Finally, In section 4.1 we discussed the 20–40 keV morphology of the emission near the   and due to the very long effective exposure of 4.7 Ms, the maps in the different energy bands revealed that 1) as the brighter and softer sources IGR J17456–2901 and 1E 1743.1–2853 become fainter with increasing energy, a hard but dim emission about 6′ from Sgr A* in the direction of positive longitudes appears, and 2) that the spectral index of this emission is quite hard and apparently qualitatively similar to that of IGR J17475–2822 (Sgr B2). This new source of soft γ-rays could well be closely related to the unidentified *Egret* source 3EG J1746–2851 and to the giant molecular cloud G 0.13-0.13.

REFERENCES

Aharonian, F. et al. 2004, A&A, 425, L13
Aharonian, F. et al. 2005a, A&A, 432, L25
Aharonian, F., et al. 2005b, Science, 307, 1938
Aharonian, F. & Neronov, A. 2005, ApJ, 619, 306
Atoyan, A., & Dermer, C. D. 2004, ApJ, 617, L123
Balick, B. & Brown, R. L. 1974, ApJ, 194, 265
Baganoff, F. K. et al. 2001, Nature, 413, 45
Baganoff, F. K. et al. 2003, ApJ, 591, 891
Bélanger, G. et al. 2004, ApJ, 601, L163
Bélanger, G. et al. 2005, ApJ, submitted
Bower, G., Yusef-Zadeh, F. & Roberts, D. 2005, ApJ, submitted
Bykov, A. M. 2002, A&A, 390, 327
Courvoisier, T. J.-L., et al. 2003, A&A, 411, L53
Crocker, R. M., et al. 2005, ApJ, in press.
Cuadra, J., et al. 2005, MNRAS, L44
Eckart, A., et al. 2004, A&A, 427, 1
Eisenhauer, F. et al. 2005, ApJ, submitted (astro-ph/0502129)
Fatuzzo, M. and Melia, F. 2003, ApJ, 596, 1035
Gaensler, B. M., Pivovaroff, M. J., & Garmire, G. P. 2001, ApJ, 556, L107
Genzel, R., & Townes, C. H. 1987, ARA&A, 25, 377
Genzel, R. et al. 2003, Nature, 425, 934
Ghez, A. M., et al. 2004, ApJ, 601, L159
Ghez, A. M. et al. 2005, ApJ, 620, 744
Goldoni et al. 1999, ApLC, 38, 305
Goldwurm, A., et al. 1994, Nature, 371, 589
Goldwurm, A. et al. 2003a, ApJ, 584, 751
Goldwurm, A. et al. 2003b, A&A, 411, L223
Goldwurm, A. et al. 2004, Proc. of 5th Integral Workshop, ESA-SP, 552, 237
Green, D. A. 2004, Bull.Astron.Soc.India 32, 335 (astro-ph/0411083)
Gros, A. et al. 2003, A&A, 411, L179
Hartman, R. C. et al. 1999, ApJS, 123, 79
Helfand, D. J. & Becker, R. H. 1987, ApJ314, 203

Jones, T. W. 1974, A&A, 30, 37
Kosack, K., et al. 2004, ApJ, 608, L97
Koyama, K. et al. 1996, PASJ, 48, 249
Knödlseder, J., et al. 2005, A&A, accepted
Lebrun, F., et al. 2003, A&A, 411, L141
Liu, S. & Melia, F. 2002, ApJ, 566, L77
Liu, S., Petrosian, V., and Melia, F. 2004, ApJ, 611, L101
Liu, S., Melia, F., and Petrosian, V. 2005, ApJ, submitted
Markoff, S., Melia, F., & Sarcevic, I. 1997, ApJ, 489, L47
Markoff, S., Melia, F., & Sarcevic, I. 1999, ApJ, 522, 870
Markoff, S., Falcke, H., Yuan, F., & Biermann, P. L. 2001, A&A, 379, L13
Maeda, Y., et al. 2002, ApJ, 570, 671
Mallet, I. et al., 1995, ApJ, 444, 222
Mayer-Hasselwander, H. et al. 1998, A & A, 335, 161
Melia, F. et al. 1998, ApJ, 508, 676
Melia, F. & Falcke, H. 2001, ARA&A, 39, 309
Muno, M. P. et al. 2004a, ApJ, 613, 326
Muno, M. P. et al. 2004b, ApJ, 613, 1179
Muno, M. P. et al. 2005a, ApJ, 622, L113
Muno, M. P. et al. 2005b, ApJ, submitted, pre-print (astro-ph/0503572)
Park, S. et al. 2004, ApJ, 603, 548
Pavlinsky, M. N., Grebenev, S. A. & Sunyaev, R. A. 1994, ApJ, 425, 110
Porquet, D. et al. 2003a, A&A, 407, L17
Porquet, D. et al. 2003b, A&A, 406, 299
Porquet, D., Decourchelle, A., & Warwick, R. S. 2003, A&A, 401, 197
Porquet, D. et al. 2005, A&A, 430, L9
Porquet, D. et al. 2005, A&A, submitted
Sidoli et al. 2004, Memorie della Societa Astronomica Italiana, 75, 507
Sidoli, L. & Mereghetti, S. 1999, A&A, 349, L49
Sakano, M. et al. 2002, ApJS, 138, 19
Sakano, M., et al. 2004, MNRAS, 350, 129
Schödel et al. 2003, ApJ, 596, 1015

Skinner, G. K. et al. 1987, Nature, 330, 544
Skinner, G. K. et al. 1990, MNRAS, 243, 72
Revnivtsev, M. G. et al. 2004, A&A, 425, L49
Tan, J. C., & Draine, B. T. 2004, ApJ, 606, 296
Terrier, R., et al. 2003, A&A, 411, L167
Tsuchiya, K. et al. 2004, ApJ, 606, L115
Ubertini, P., et al. 2003, A&A, 411, L131
Winkler, C. 2003, A&A, 411, L1
Yuan, F., Markoff, S., & Falcke, H. 2002, A&A, 383, 854

Yuan, F., Quataert, E., & Narayan, R. 2003, ApJ, 598, 301
Yusef-Zadeh, F. et al. 1996, ApJ, 466, L25
Yusef-Zadeh, F., Choate, D. & Cotton, W. 1999, ApJ, 518, L33
Yusef-Zadeh, F., Melia, F., & Wardle, M. 2000, Science, 287, 85
Yusef-Zadeh, F. et al. 2002, ApJ, 568, L121
Yusef-Zadeh, F., Hewitt, J. W., & Cotton, W. 2004, ApJS, 155, 421